



## Structural and Ammonia Adsorption Properties of the Gördes Clinoptilolite After HCl Acid Treatment

Orkun ERGURHAN , Burcu ERDOGAN\* 

*Eskişehir Technical University, Department of Physics, 26470, Eskişehir, Türkiye*

### Highlights

- NH<sub>3</sub> uptake was investigated at 298 K using a volumetric device.
- Characterization of samples were investigated by XRD, XRF, SEM and N<sub>2</sub> adsorption.
- CLN had the highest ammonia uptake (5.01 mmol.g<sup>-1</sup>).

### Article Info

*Received: 07 June 2023*

*Accepted: 21 Mar 2024*

### Keywords

*Adsorption  
Ammonia  
Acid treatment  
Clinoptilolite  
Zeolite*

### Abstract

The effect of activation with HCl on the ammonia adsorption characteristics of natural Gördes clinoptilolite was studied in order to evaluate the usability of this mineral in various environments where ammonia removal is required, such as livestock facilities. Clinoptilolite was treated with HCl solutions (0.5, 1.0, 1.5, 2.0, 2.5 and 3.0 M) at 90°C for 4 h. XRD, XRF, FT-IR, TGA, DTA and N<sub>2</sub> adsorption techniques were used for structural and thermal characterization of the adsorbents. NH<sub>3</sub> adsorption isotherms were measured volumetric analysis at 298 K up to 100 kPa. Acid activation not only caused textural and structural changes such as removal of exchangeable cations but also affected the thermal behavior and gas retention of the clinoptilolite. Nitrogen adsorption results showed that it is possible to improve the specific surface area and micropore area values of clinoptilolite with acid activation up to 1.5 M. In addition, the NH<sub>3</sub> adsorption capacities of clinoptilolite samples (4.33-5.01 mmol.g<sup>-1</sup>) were compared with the ammonia removal data of natural and synthetic zeolites (1.77 - 9.32 mmol.g<sup>-1</sup>) reported in previous studies.

## 1. INTRODUCTION

The agricultural and livestock sector is one of the most indispensable parts of society in the 21st century. Thanks to them, billions of us can find food in our local supermarkets. But as with all technological conveniences, we pay the price for this convenience in the form of air pollution. The quality of the air indoors and outdoors is becoming more and more important [1]. Many studies have shown that indoor volatile compounds can cause medical problems such as irritation of mucous membranes [2]. Ammonia, a colorless, malodorous and dangerous gas, is one of the air pollutants [3-5]. It consists of one nitrogen and three hydrogen atoms. Ammonia has a molar mass of 17.0312 g/mol and a Debye dipole moment of 1.5 due to its asymmetric shape [5]. The concentration of ammonia in pig farms can affect the growth and health of the animals. For example, an inflammatory response has been observed in the respiratory system of pigs exposed to ammonia concentrations of 100 and 150 ppm [6]. Furthermore, 100-400ppm ammonia causes eye and throat irritation in humans [7]. Respiratory symptoms are reversible. However, chronic bronchitis has been reported in some cases [8]. Livestock and agricultural activities also cause more ammonia emissions than fuel combustion, vehicles and all industrial activities [9]. Sensitive crops and human health are directly affected by atmospheric concentrations of ammonia [10]. Therefore, ammonia emissions from livestock farms and agricultural land need to be controlled and zeolites may be good candidates for these applications.

Zeolites are alumina-silicate minerals that have been known for almost three centuries [11]. Their crystalline framework is based on simple tetrahedral blocks (TBs) with the general formula TO<sub>4</sub>. Here O refers to oxygen and T can be silicon or aluminum. TBs combine to form three-dimensional networks containing cavities, channels, exchangeable framework cations and water [12]. In addition, the different

\*Corresponding author, e-mail: burcuerdogan@eskisehir.edu.tr

ways in which these TBs can be linked give rise to more than fifty types of natural zeolites found in nature [11-13]. Clinoptilolite is a member of the heulandite (HEU) group. The general formula of clinoptilolite can be given as  $(\text{Na,K})_6(\text{Al}_6\text{Si}_{30}\text{O}_{72}) \cdot 20\text{H}_2\text{O}$ . Unit cell parameters are  $a=17.62 \text{ \AA}$ ,  $b=17.91 \text{ \AA}$ ,  $c=7.39 \text{ \AA}$  and  $\beta = 116^\circ 16'$ . Its framework structure with monoclinic  $C2/m$  symmetry is almost identical to that of heulandite [13]. However, clinoptilolite has greater structural stability than heulandite at high temperatures. Therefore, Mumpton defines clinoptilolite as a zeolite that survives overnight heating at  $450 \text{ }^\circ\text{C}$  [14]. Clinoptilolite has a 2D channel system consisting of three channels. Channels A and B lie along the  $c$ -axis and channel C intersects these channels along the  $a$ -axis. Thus, the structure has no channel along the  $b$ -axis, matter transfer in clinoptilolite occurs only along the  $a$ - and  $c$ -axes. Channel A is the largest tunnel with a 10-membered ring in the clinoptilolite structure. Channels B and C consist of 8-membered rings and are relatively smaller than channel A [11,13]. Clinoptilolite has four cation sites in these channels, named M(1), M(2), M(3) and M(4) (Figure 1). M(1) site is channel A. Normally  $\text{Na}^+$  and  $\text{Ca}^{2+}$  cations are found at this site. M(4) is in the center of channel A and contains the  $\text{Mg}^{2+}$  cation coordinated with  $\text{H}_2\text{O}$  molecules. The M(2) site is located in channel B and is usually occupied by  $\text{Ca}^{2+}$ , and finally, the M(3) region is in the center of the C channel and there are  $\text{K}^+$  ions in this region. Besides these well-known sites, there are studies showing that clinoptilolite can have other cation positions containing  $\text{Cs}^+$ ,  $\text{Ag}^+$ ,  $\text{Pb}^{2+}$ ,  $\text{Cd}^{2+}$ ,  $\text{Hg}^{2+}$  ions [15-18]. Clinoptilolite can be used for gas separation and removal of toxic gases due to its structural advantages [19-24].

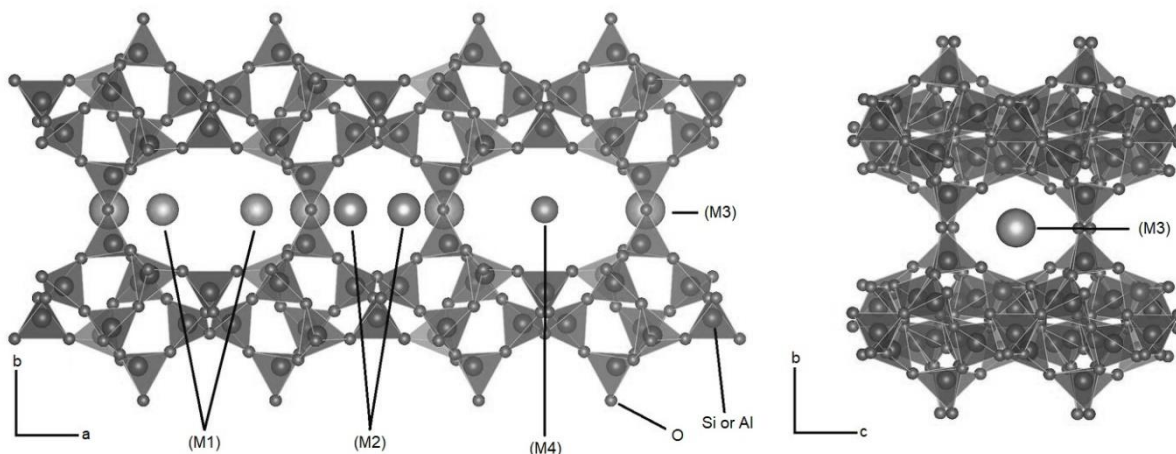


**Figure 1.** View of clinoptilolite framework and cation sites along  $c$ -axis (a) and  $a$ -axis (b)

Prior to gas adsorption applications, it may be necessary to modify and optimize the structure of the clinoptilolite. Therefore, applications such as cation exchange and acid activation are common [18,25]. Acid activation increases the BET surface area [26] and the number of acid sites of clinoptilolite [27] and opens blocked channels [28] by dealumination and replacement of  $\text{H}^+$  ions with exchangeable cations. On the other hand, increasing acid concentrations can cause the crystal structure of clinoptilolite to collapse [29]. A number of studies have been conducted which investigate the adsorption of ammonia on natural and synthetic zeolites [3,4,30-37]. However, the effect of activating clinoptilolite with different concentrations of HCl solutions on ammonia adsorption applications has not been investigated. This study was conducted with the objective of examining the impact of acid activation on ammonia removal by clinoptilolite in environments such as the poultry and cattle industry.

## 2. MATERIAL METHOD

### 2.1. Materials and Chemicals

Clinoptilolite (CLN) from Gördes was used in  $<63 \mu\text{m}$  fractions. The clinoptilolite samples were then stirred in deionized water at  $50^\circ\text{C}$  for 4 h to eliminate soluble impurities from the structure. Acid-treated forms of clinoptilolite were prepared to compare the physicochemical and gas adsorption characteristics. First, five grams of clinoptilolite were treated with HCl solutions (0.5-3.0 M) at  $90 \text{ }^\circ\text{C}$  for 4 h. The solution mixtures containing clinoptilolite were then filtered, washed repeatedly with deionised water at boiling

temperature and dried at 110 °C for 24 h. The resulting samples were labelled CLN-HX, where X indicates the acid molarity. HCl was supplied by Merck.

## 2.2. Experimental

A chemical analysis was conducted on powdered samples fused with lithium tetraborate using X-ray fluorescence spectroscopy (Rigaku ZSX Primus instrument). Loss of Ignition (LOI) was quantified by mass measurement following the samples' heating to 1000°C at a rate of 10°C per minute, a period of one hour, and subsequent cooling to room temperature at the same rate. Powder XRD patterns of the samples were collected using Bruker D8 Advance device operating with  $\text{CuK}\alpha$  ( $\lambda = 1.5406 \text{ \AA}$ ) in the range of  $2\theta$  values 5-40° and step range of 0.02°. DTA and TG analyses were carried out on a Setaram Setsys Evolution equipment from 30 to 1000 °C at a heating rate of 10 °C min<sup>-1</sup>. For TG-DTA analyses, approximately 35 mg of the sample was employed as the carrier gas was N<sub>2</sub>. The conventional KBr pellet technique was used for FT-IR analysis. First of all, the samples and KBr were kept in an oven at 100 °C for 3 h. Then, 0.5 mg sample was added into 200 mg KBr and mixed in agate mortar until it became homogeneous. The KBr-sample mix was then pressed with a desktop size manual hydraulic press under a load of 2 Tons for approximately 2 min. The clinoptilolite samples for which ammonia adsorption measurements were completed were directly mixed with KBr and pressed under the same conditions. FT-IR spectra were obtained using a BRUKER Vertex 80v spectrometer at 4 cm<sup>-1</sup> resolution, with 16 scan times in the 400-4000 cm<sup>-1</sup> wavelength range. All spectral data were collected with an RT-DLaTGS detector at room temperature. The adsorption and desorption of nitrogen (N<sub>2</sub>) were evaluated via a Micromeritics 3FLEX analyzer at 77 K. The specific surface areas ( $S^{\text{BET}}$ ) were determined by BET equation ( $0.05 < P/P_0 < 0.35$ ). Micropore surface areas ( $S^{\mu\text{P}}$ ) and volumes ( $V^{\mu\text{P}}$ ) were determined using the t-plot method. NH<sub>3</sub> isotherms were measured at 298 K up to 100 kPa using Micromeritics 3Flex instrument. Prior to the N<sub>2</sub> and NH<sub>3</sub> adsorption experiments, the clinoptilolites were outgassed at 300 °C for 10 h.

## 3. THE RESEARCH FINDINGS AND DISCUSSION

### 3.1. Elemental Analysis

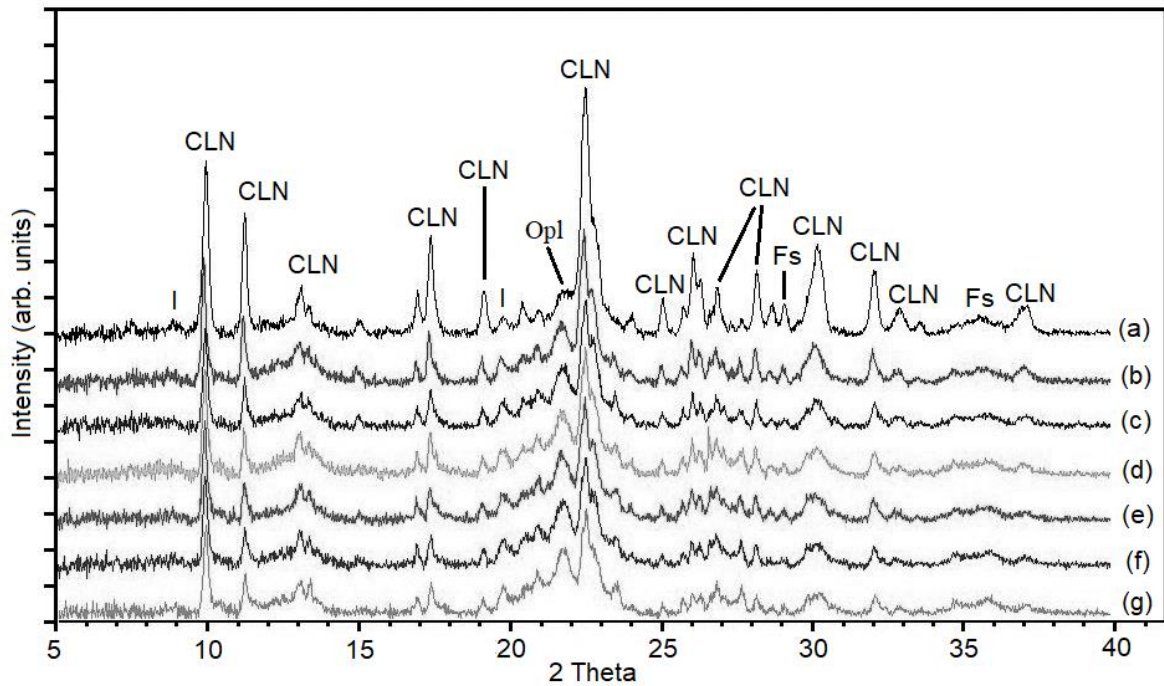
The elemental analysis of the clinoptilolites are given in Table 1. The CLN sample is characterized by high K<sub>2</sub>O and CaO and low Na<sub>2</sub>O and MgO. Even activation with 0.5 M acid was found to be sufficient for significant dealumination and the replacement of H<sup>+</sup> ions by exchangeable cations (Na<sup>+</sup>, K<sup>+</sup>, Ca<sup>2+</sup> and Mg<sup>2+</sup>). However, a complete dealumination could not be achieved at the acid concentrations used. Owing to the acid treatment, the extra-framework cations and framework Al<sup>3+</sup> were progressively removed and free amorphous silica, insoluble in the acid solution, was obtained. The SiO<sub>2</sub>/Al<sub>2</sub>O<sub>3</sub> ratio increased from 5.64 for CLN to 11.66 for the 3.0 M HCl treated sample. The K<sup>+</sup> and Ca<sup>2+</sup> remaining in the acid treated forms would correspond to the illite and feldspar remaining in the material as shown by the XRD patterns (Figure 2). Previous studies also found a similar effect of acid activation on the elemental composition of clinoptilolite [26,38,39].

### 3.2. X-ray Diffraction

The powder XRD patterns of the clinoptilolite samples (raw, CLN-H0.5, CLN-H1.0, CLN-H1.5, CLN-H2.0, CLN-H2.5, CLN-H3.0) forms are shown in Figure 2. According to the results, the main clinoptilolite reflections were observed at  $2\theta = 9.91^\circ, 19.15^\circ, 22.51^\circ, 28.20^\circ, 30.22^\circ$  with corresponding distances of 8.91 Å, 4.65 Å, 3.95 Å, 3.16 Å and 2.96 Å, respectively [40]. CLN contains 80-85% clinoptilolite as the main mineral. It also contains impurities such as opal-CT (5-6%), illite (2%), feldspar (3%) and amorphous matter (5-10%) according to the method of Esenli and Sirkecioğlu, 2005 [41]. Increasing acid molarity caused a gradual decrease in the intensity of the clinoptilolite peaks and the formation of a broad baseline between 19 and 30° of  $2\theta$ . These are indicative of the partial collapse of the structure and the formation of an amorphous phase. Similar broad backgrounds due to acid activation have been reported in previous studies [39]. However, illite and feldspar peaks are still present in the sample activated with 3.0 M HCl solution, indicating that the illite and feldspar are more resistant to acid attack than the clinoptilolite.

**Table 1.** Chemical analyses in oxides (%) for the clinoptilolite samples

Sample	SiO <sub>2</sub>	Al <sub>2</sub> O <sub>3</sub>	Fe <sub>2</sub> O <sub>3</sub>	Na <sub>2</sub> O	K <sub>2</sub> O	CaO	MgO	LOI
CLN	70.5	12.5	1.17	0.468	5.08	2.20	0.573	7.42
CLN-H0.5	80.0	8.77	1.13	-	2.97	0.467	0.399	6.28
CLN-H1.0	81.4	8.14	1.09	-	2.20	0.460	0.350	6.19
CLN-H1.5	81.3	7.64	1.08	-	1.78	0.411	0.380	7.25
CLN-H2.0	82.1	7.73	0.987	-	1.64	0.410	0.410	6.30
CLN-H2.5	82.4	7.28	0.931	-	1.50	0.418	0.372	6.69
CLN-H3.0	82.6	7.08	0.974	-	1.43	0.399	0.332	6.95

**Figure 2.** XRD patterns of CLN (a), CLN-H0.5 (b), CLN-H1.0 (c), CLN-H1.5 (d), CLN-H2.0 (e), CLN-H2.5 (f) and CLN-H3.0 (g) (CLN: clinoptilolite, Opl: opal, Fs: feldspar, I: illite)

### 3.3. Thermal Properties

The DTA and TG curves obtained for the clinoptilolites are shown in Figure 3. Strong endothermic peaks at 68 °C and 153 °C on the DTA curve of CLN with the largest mass loss of 2.48% between 30 and 200 °C are owing to dehydration of the loss of water located in the voids and bound to the extra-framework cations. For temperatures between 200 and 600 °C, the mass loss is 4.34%. Between 600 and 800 °C, the remainder of the strongly associated water is gradually eliminated with a mass loss of 0.49% due to dehydroxylation. As seen from Figure 3, the clinoptilolite samples presented the continuous mass loss curves. It was found that the thermal properties of clinoptilolite samples varied in terms of both the SiO<sub>2</sub>/Al<sub>2</sub>O<sub>3</sub> ratio and the extra-framework cation composition. The mass losses for the acid activated clinoptilolites (7.19 - 7.41%) were lower than those for the CLN (7.45%). In addition, the intensity of the first two endothermic peaks gradually decreased in the acid modified forms. These results may be related to the dealumination and the elimination of the non-framework cations (Table 1).



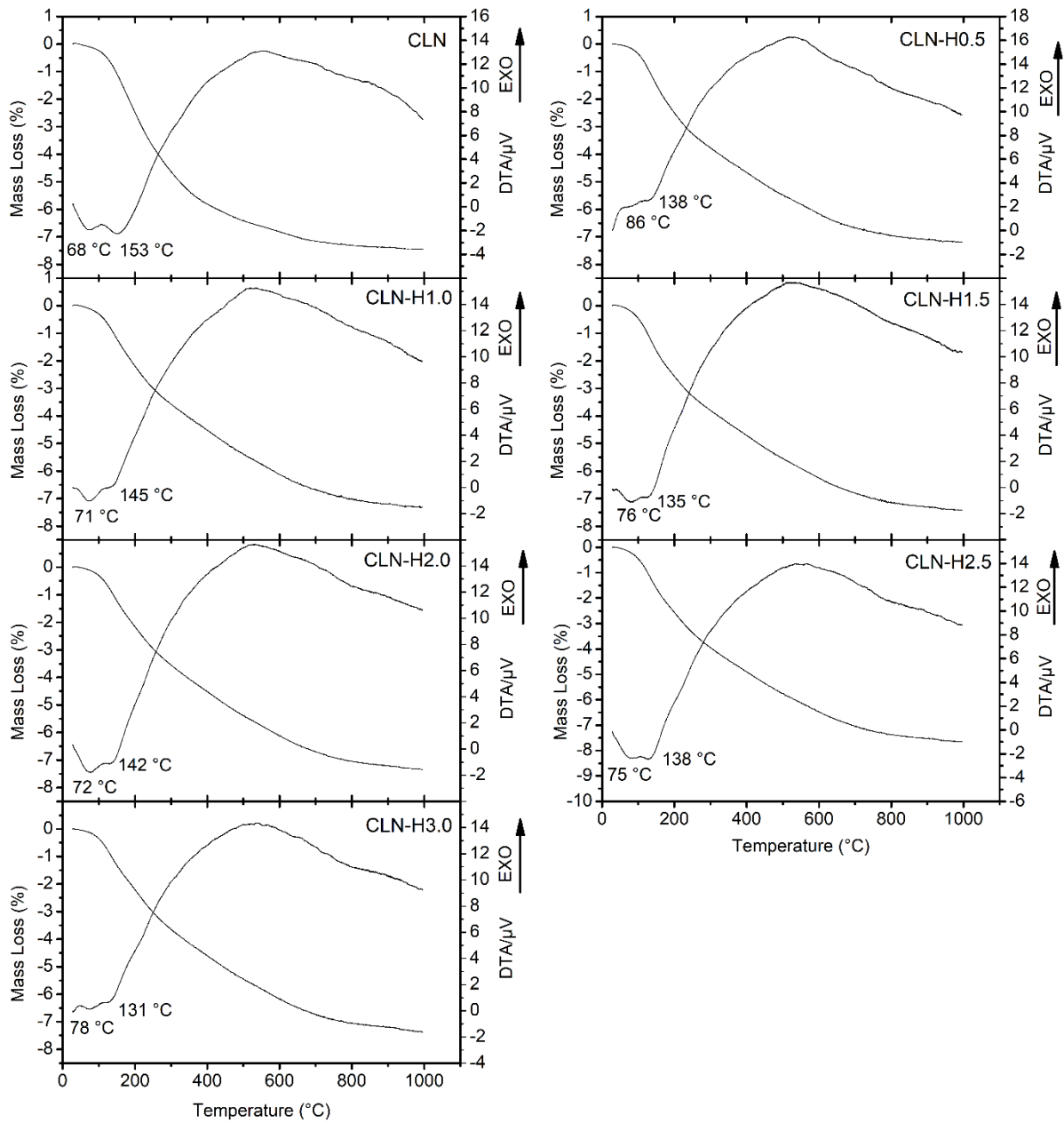


**Figure 3.** TG/DTA curves of the raw and acid-activated clinoptilolites

As the majority of the water in the structural cavities is bound to non-framework cations, the dehydration of natural zeolites is contingent upon the presence of additional framework cations, with particular emphasis placed on their hydration energy. Natural clinoptilolites containing cations with high hydration energies contain significantly more water and retain this water up to higher temperatures.

### 3.4. FT-IR

Figure 4 presents the FT-IR spectra of all clinoptilolites. The characteristic vibrations of the clinoptilolite structure can be seen between 400-1200  $\text{cm}^{-1}$ . The 420-500  $\text{cm}^{-1}$  vibrations are associated with internal tetrahedral T-O bending mode. The 605  $\text{cm}^{-1}$  band is the result of external tetrahedral double ring vibrations. The strongest band at 1050  $\text{cm}^{-1}$  belongs to the external tetrahedral linkage asymmetric stretching mode [42,43]. After acid treatment, the band at 1051  $\text{cm}^{-1}$  shifted to a higher frequency at 1084  $\text{cm}^{-1}$  owing to dealumination and partial breakdown of the clinoptilolite framework [38,44]. Partial structural breakdown and dealumination can also be observed from the relative changes in bands around 467 and 605  $\text{cm}^{-1}$ . The

intensity of the clinoptilolite fingerprint band at  $605\text{ cm}^{-1}$ , which represents the amount of clinoptilolite in the tuff, decreases with acid treatment, while the characteristic amorphous silica band at  $460\text{ cm}^{-1}$  and  $795\text{ cm}^{-1}$  increases. This indicates the formation of amorphous silica, which is also seen in the XRD data (Figure 2) [39]. The band at  $1638\text{ cm}^{-1}$  is related to O-H bending vibrations of water [45]. The vibrational bands around  $3434$  and  $3630\text{ cm}^{-1}$  reflect the Si-OH groups and bridging hydroxyls (Si-O(H)-Al), respectively [46]. After ammonia adsorption, the FT-IR spectrum of the clinoptilolite structure remains almost the same, but a band appears at around  $1400\text{ cm}^{-1}$ . Ammonium formation is a known phenomenon in ammonia-zeolite interactions [47-49]. This band can therefore be attributed to the  $\nu_4$  stretching vibrational mode of the ammonium ion [50,51].

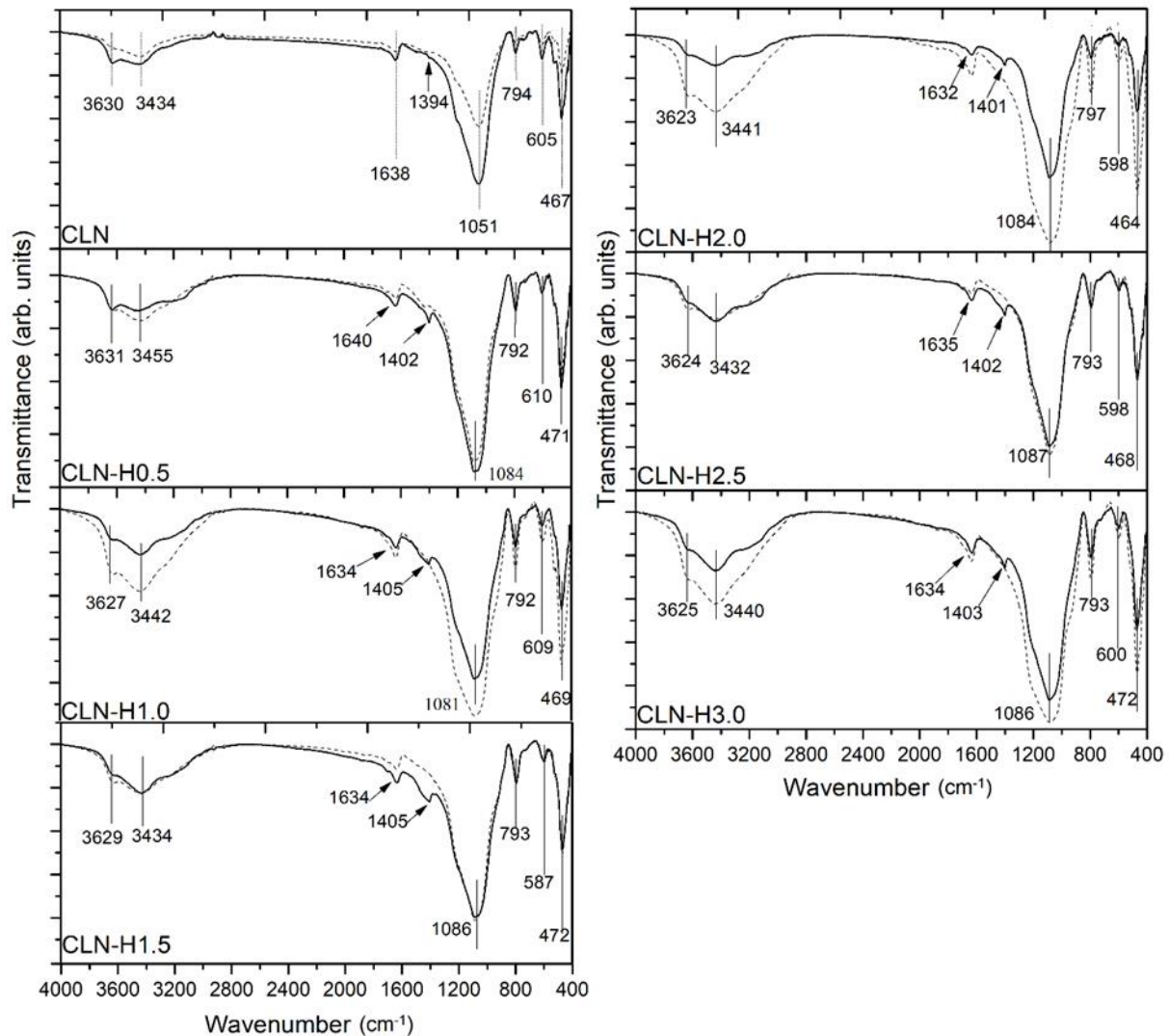


**Figure 4.** FT-IR spectra of the raw and acid-activated clinoptilolites before (dashed line) and after (solid line) the ammonia adsorption

### 3.5. N<sub>2</sub> Adsorption

N<sub>2</sub> adsorption-desorption isotherms for all the clinoptilolite samples are given in Figure 5 and their textural characteristics are tabulated in Table 2. All isotherms are of type IV and have a hysteresis loop associated with pore condensation [52]. As seen from the shape of the isotherms, the clinoptilolite sample contains micropores (pore width < 2 nm) in addition to mesopores (pore width in the range 2-50 nm). The initial part of the isotherms can be attributed to monolayer-multilayer adsorption [52]. The specific surface area of the sample increased from  $42\text{ m}^2\cdot\text{g}^{-1}$  for CLN to  $178\text{ m}^2\cdot\text{g}^{-1}$  for CLN-H1.5.

This increase in the BET surface area is owing to partial loss of extra-framework cations, dissolution of aluminum, elimination of pore-blocking impurities and formation of secondary porosity due to dissolution of free bonds. Both the BET surface area and microporous surface area values decreased in activated samples with acid molarity greater than 1.5 M. The CLN-H3.0 sample had the lowest specific surface area ( $163 \text{ m}^2.\text{g}^{-1}$ ) and microporous surface area ( $113.97 \text{ m}^2.\text{g}^{-1}$ ) among the acid modified forms.

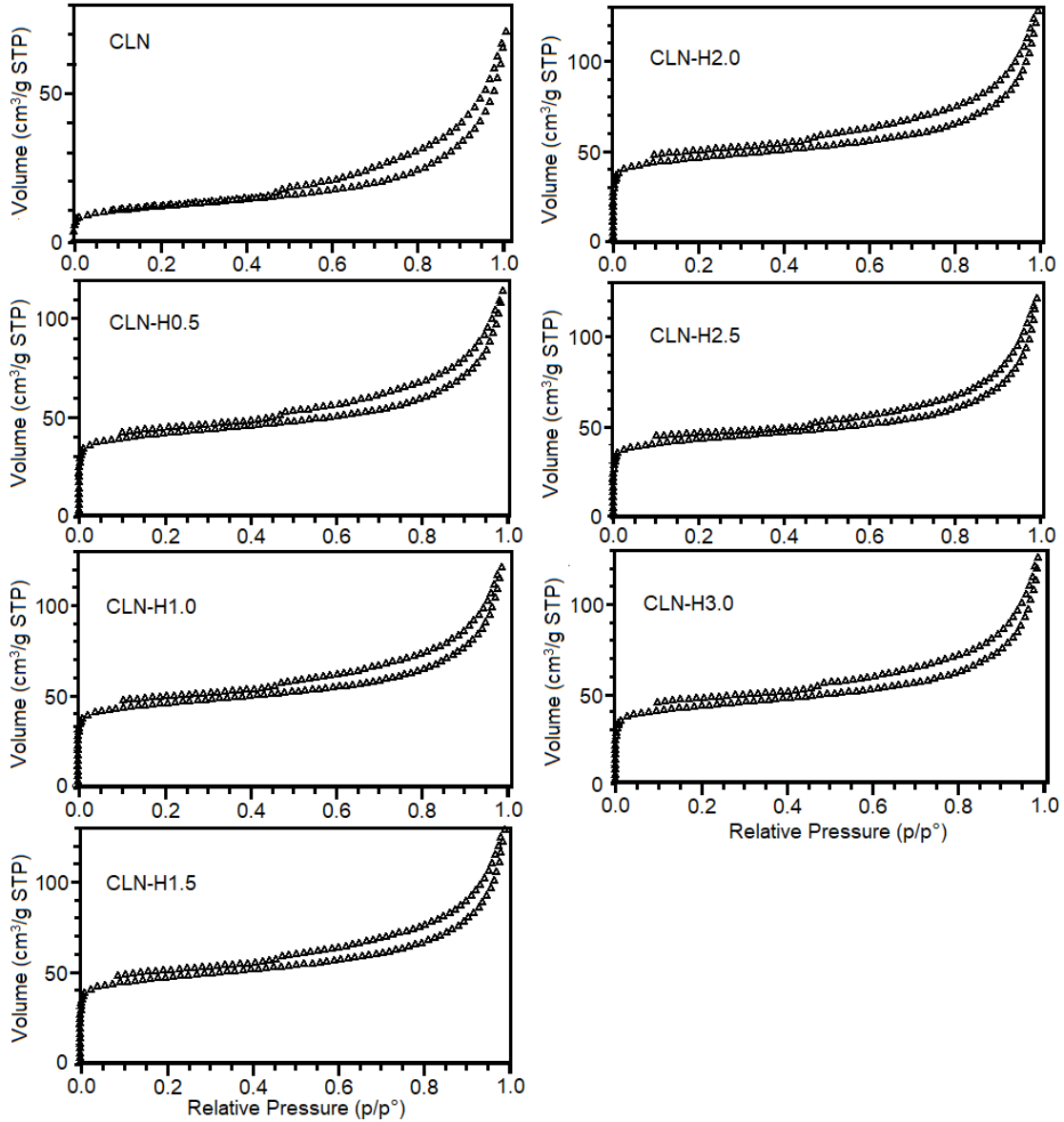


**Figure 5.** Nitrogen adsorption isotherms of raw and acid activated clinoptilolite

**Table 2.**  $N_2$  data of the raw and acid activated clinoptilolites

Sample	$S_{BET}$ ( $\text{m}^2.\text{g}^{-1}$ )	$S_{\mu^P}$ ( $\text{m}^2.\text{g}^{-1}$ )	$V_{\mu^P}$ ( $\times 10^{-2} \text{ cm}^3.\text{g}^{-1}$ )
CLN	42	11.99	0.49
CLN-H0.5	157	112.18	4.58
CLN-H1.0	173	127.50	5.18
CLN-H1.5	178	129.35	5.30

CLN-H2.0	175	125.97	5.15
CLN-H2.5	165	122.30	4.91
CLN-H3.0	163	113.97	4.66

This result for CLN-H3.0 sample, where the acid was used at the highest molarity, can be attributed to the fact that delamination and partial destruction of the clinoptilolite crystal structure occurs at the highest rate due to acid activation compared to other acid modified forms. This finding is consistent with the XRF results (Table 1), XRD (Figure 2.) and FT-IR (Figure 4.) analyses.

### 3.6. NH<sub>3</sub> Adsorption

Ammonia adsorption isotherms and absolute uptake for clinoptilolite samples at 298 K to 100 kPa are given in Figures 6 and 7 and Table 3. According to the classification given by IUPAC, the isotherms are of type I. NH<sub>3</sub> isotherms are generally observed on microporous materials like activated carbons, certain porous oxides and zeolites [52]. At relatively low pressures, high adsorption amounts are observed due to the high adsorption potential and narrow pore diameter. However, at relatively high pressures, the adsorption value approaches a constant. This indicates that the accessible micropore volume exerts a more pronounced influence on the adsorption process than the internal surface area [52,53].

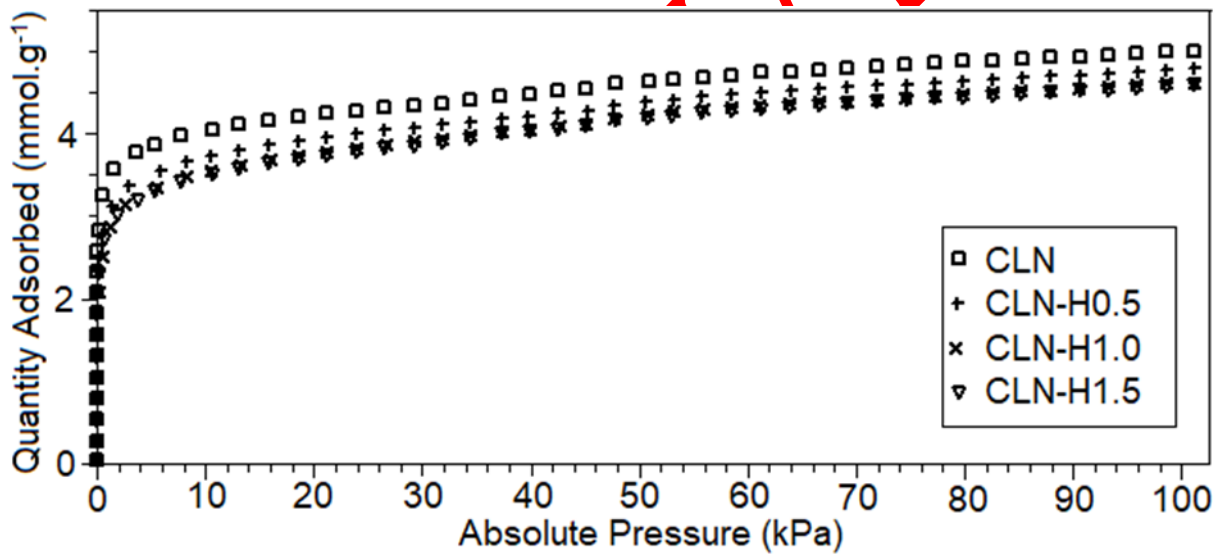


Figure 6. NH<sub>3</sub> adsorption isotherms of CLN, CLN-H0.5, CLN-H1.0 and CLN-H1.5 samples



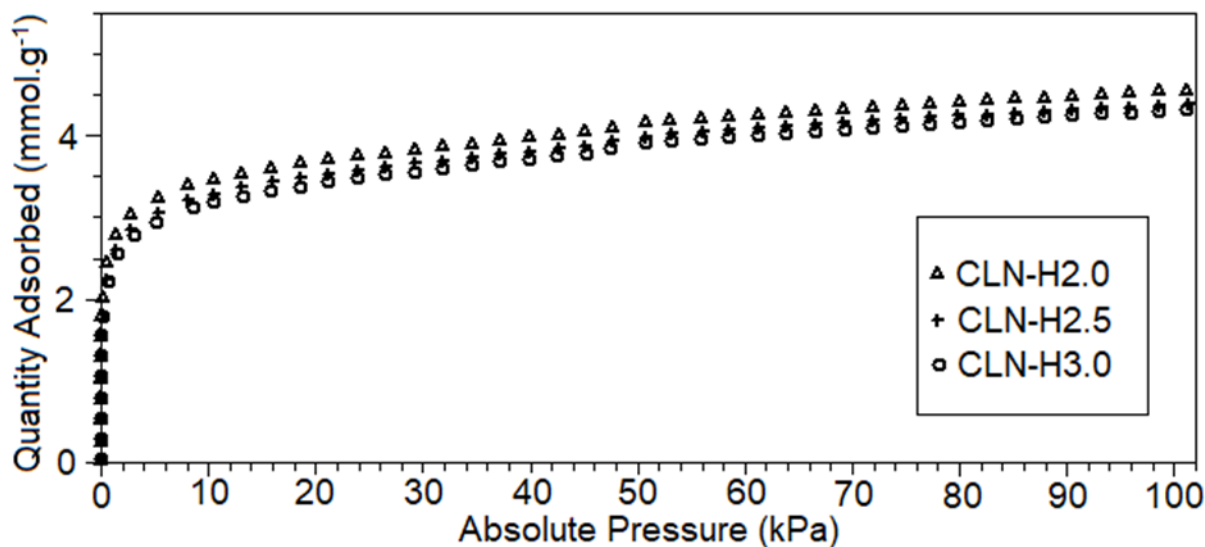


Figure 7.  $\text{NH}_3$  adsorption isotherms of CLN-H2.0, CLN-H2.5 and CLN-H3.0 samples

The  $\text{NH}_3$  molecule has a kinetic diameter of 0.26 nm can easily diffuse through the pores of clinoptilolite. In this study, the ammonia uptake decreased in the order  $\text{CLI} > \text{CLI-H0.5} > \text{CLI-H1.0} > \text{CLI-H1.5} > \text{CLI-H2.0} > \text{CLI-H2.5} > \text{CLI-H3.0}$  (Figures 6 and 7). The maximum uptake of ammonia is exhibited by CLN ( $5.01 \text{ mmol.g}^{-1}$ ) and the minimum by CLN-H3.0 ( $4.33 \text{ mmol.g}^{-1}$ ). Although all acid-treated forms have higher surface area values ( $157\text{-}178 \text{ m}^2.\text{g}^{-1}$ ) than the raw sample CLN ( $42 \text{ m}^2.\text{g}^{-1}$ ), the adsorption capacities of these samples are lower ( $4.33\text{-}4.79 \text{ mmol.g}^{-1}$ ) than that of raw CLN ( $5.01 \text{ mmol.g}^{-1}$ ), because of the removal of exchangeable cations and the consequent reduction in the local electric field. In addition to changes in structure due to acid modification and dealumination, this clearly demonstrates the effect of removal of extra framework cations on ammonia adsorption. As ammonia is a highly polar molecule, it tends to share a lone pair of electrons with these exchangeable cations. At high pressures, however, the number of polar molecules adsorbed is directly related to the cation density in the framework [54]. In acid-treated samples, the ammonia uptake decreased with increasing acid molarity. The variation in ammonia gas adsorption capacity for natural clinoptilolite and its acid-treated forms indicated that the electrostatic and the dispersion forces played the role in the adsorption. Acid modification resulted in the exchange of the exchangeable cations with  $\text{H}^+$  cations [55,56]. Due to the dealumination process, the number of permanent negative sites in the clinoptilolite structure decreased and the zeolite surface became less negative [55,57]. The high affinity of sample CLN for  $\text{NH}_3$  is therefore due to the interactions of the permanent dipole moment (1.47 Debye) of ammonia molecule with the electric field generated by cations in the clinoptilolite. As shown in Table 3, the uptake of ammonia by sample CLN ( $5.01 \text{ mmol.g}^{-1}$ ) was higher than that of natural ( $0.63 \text{ mmol.g}^{-1}$ ) and acid-treated clinoptilolite ( $1.12\text{-}1.27 \text{ mmol.g}^{-1}$ ) from the Ninny deposit, Hrabovec [34], dealuminated faujasite from Wessalith DAY F20 ( $1.77 \text{ mmol.g}^{-1}$ ) [35], clinoptilolite ( $0.72 \text{ mmol.g}^{-1}$ ) [31], clinoptilolite ( $1.01 \text{ mmol.g}^{-1}$ ) [32], clinoptilolite (Slovakia) ( $0.71 \text{ mmol.g}^{-1}$ ) [58] and lower than a clinoptilolite-rich tuff from Thrace, NE Greece ( $5.28 \text{ mmol.g}^{-1}$ ) [33] and clinoptilolite from Mud Hills CA ( $5.90 \text{ mmol.g}^{-1}$ ) [35]. These findings demonstrate that the origin, mineral composition, cationic content, and impurity concentration of natural clinoptilolite have a significant impact on the capacity of this material to retain ammonia because natural clinoptilolite has a different mineralogical and chemical composition depending on the mineral deposit from which it was formed and mined. Furthermore, CLN showed lower ammonia adsorption capacity than 13X zeolite Baylith WE894 ( $9.32 \text{ mmol.g}^{-1}$ ) [35], 5A Lancaster 5830 ( $7.81 \text{ mmol.g}^{-1}$ ) [35], 4A Baylith TG242 ( $8.71 \text{ mmol.g}^{-1}$ ) [35], silica gel 40 Fluka 60736 ( $6.25 \text{ mmol.g}^{-1}$ ) [35], due to textural and structural differences. Synthetic zeolites generally have a higher gas retention than natural ones owing to their uniform structure, but are more expensive [59]. In addition, the abundance of the clinoptilolite type natural zeolites and their high sorption capacities provide cost effective and environmentally friendly solutions for gas adsorption applications.

**Table 3.** Comparison of NH<sub>3</sub> adsorption capacities of the present work with literature data at 298 K

Sample	Pressure (kPa)	NH <sub>3</sub> Adsorption Capacity (mmol.g <sup>-1</sup> )	Reference
CLN	101	5.01	Present Study
CLN-H0.5		4.79	
CLN-H1.0		4.62	
CLN-H1.5		4.59	
CLN-H2.0		4.58	
CLN-H2.5		4.39	
CLN-H3.0		4.33	
Clinoptilolite	101	~1.01 (14.155 mg N g <sup>-1</sup> )	[31]
Clinoptilolite	101	~0.72 (10.10 mg N g <sup>-1</sup> )	[32]
Clinoptilolite-rich tuff Pentalofos, Greece	101	~5.28	[33]
Clinoptilolite treated with 1.0 M Mg(NO <sub>3</sub> ) <sub>2</sub>	101	5.37	[58]
Natural Clinoptilolite from Nizny Hrabovec	101	0.63	[34]
pre-treated with 30 % H <sub>2</sub> SO <sub>4</sub>	101	1.27	
pre-treated with 30 % H <sub>3</sub> PO <sub>4</sub>	101	1.17	
pre-treated with 30 % HNO <sub>3</sub>	101	1.12	
Clinoptilolite (USA)	101	5.90	[35]
Faujasite dealuminated	101	1.77	
Pentasil dealuminated	101	2.34	
4A zeolite (Baylith TG242)	101	8.71	
5A zeolite (Lancaster 5830)	101	7.81	
13X zeolite (Baylith WE894)	101	9.32	
Alumina (LaRoche 1597)	101	3.01	
Silica gel 40	101	6.25	
Clinoptilolite (Slovakia)	fixed bed	0.71 / (12.2 mg g <sup>-1</sup> )	[58]

Many studies in the literature have investigated ammonia adsorption on natural and synthetic zeolites [3,4,30-37]. The innovative aspect of this study is to examine the influence of activating Gördes clinoptilolite with different concentrations of HCl solution on ammonia adsorption applications. As a result, Raw CLN, which has the highest ammonia adsorption capacity among the samples used in this study, was found to be a suitable material for ammonia gas removal.

#### 4. CONCLUSIONS

In this study, Gördes clinoptilolite was investigated to determine the influence of HCl activation on its physicochemical and ammonia adsorption characteristics. Due to the dealumination and partial dissolution of the crystal structure, with increasing acid concentration the peak intensities of clinoptilolite decreased. As a result of the treatment with HCl acid, it was determined that there were notable alterations in the elemental composition of the clinoptilolite and in the  $\text{SiO}_2/\text{Al}_2\text{O}_3$  ratio (from 5.64 to 11.66). The transmittance at  $605\text{ cm}^{-1}$ , the characteristic band related to clinoptilolite content, decreased with increasing acid concentration. Acid activation up to 1.5 M improved both microporosity and specific surface areas, but acid treatment with HCl did not increase the ammonia uptake of Gördes clinoptilolite. The decrease in gas adsorption capacity of the acid-treated clinoptilolites indicated the effect of the removal of exchangeable cations on  $\text{NH}_3$  affinity. Therefore, The results indicated that the ammonia uptake of the samples is dependent on the type and number of cations present in the channels, rather than the BET surface area. The higher ammonia uptake of CLN ( $5.01\text{ mmol.g}^{-1}$ ), a raw sample from the Gördes region, compared to acid-treated forms ( $4.33\text{-}4.79\text{ mmol.g}^{-1}$ ) can be recommended for ammonia removal in poultry houses and livestock industries without additional HCl acid treatment.

#### ACKNOWLEDGMENTS

The financial support of the Commission of Scientific Research Project of Eskisehir Technical University under the grant number 20ADP225 is gratefully acknowledged.

#### CONFLICTS OF INTEREST

No conflict of interest was declared by the authors.

#### REFERENCES

- [1] Kampa, M., and Castanas, E., "Human health effects of air pollution", *Environmental Pollution*, 151(2): 362-367, (2008).
- [2] Lindgren, T., "A case of indoor air pollution of ammonia emitted from concrete in a newly built office in Beijing", *Building and Environment*, 45(3): 596-600, (2010).
- [3] Ciahotný, K., Melenová, L., Jirglová, H., Pachtová, O., Kočířík, M., and Eić, M., "Removal of ammonia from waste air streams with clinoptilolite tuff in its natural and treated forms", *Adsorption*, 12: 219-226, (2006).
- [4] Li, X., Lin, C., Wang, Y., Zhao, M., and Hou, Y., "Clinoptilolite adsorption capability of ammonia in pig farm", *Procedia Environmental Sciences*, 2: 1598-1612, (2010).
- [5] Max, A., Ammonia, 1. Introduction. In C. Ley (Ed.), *Ullmann's encyclopedia of industrial Chemistry*, Wiley-VCH Verlag GmbH & Co. KGaA, 1-54, (2011).
- [6] Drummond, J. G., Curtis, S. E., Simon, J., and Norton, H. W., "Effects of aerial ammonia on growth and health of young pigs", *Journal of Animal Science*, 50(6): 1085-1091, (1980).
- [7] Ryer-Powder, J. E., "Health effects of ammonia", *Plant/Operations Progress*, 10(4): 228-232, (1991).

- [8] World Health Organization: "Ammonia. Environ Health Critter", 54: 1– 210, (1986)
- [9] McCubbin, D. R., Apelberg, B. J., Roe, S., and Divita, F., "Livestock ammonia management and particulate-related health benefits", *Environmental Science & Technology*, 36(6): 1141-1146, (2002).
- [10] Sutton, M. A., van Dijk, N., Levy, P. E., Jones, M. R., Leith, I. D., Sheppard, L. J., Leeson, S., Sim, T. Y., Stephens, A., Braban, C. F., Dragosits, U., Howard, C. M., Vieno, M., Fowler, D., Corbett, P., Naikoo, M. I., Munzi, S., Ellis, C. J., Chatterjee, S., Steadman, C. E., Möring, A., and Wolseley, P. A., "Alkaline air: changing perspectives on nitrogen and air pollution in an ammonia-rich world", *Philosophical Transactions of the Royal Society A*, 378(20183): 20190315, (2020).
- [11] Passaglia, E., and Sheppard, R. A., "The Crystal Chemistry of Zeolites", *Reviews in Mineralogy and Geochemistry*, 45(1): 69-116, (2001).
- [12] Elaiopoulos, K., Perraki, T., and Grigoropoulou, E., "Monitoring the effect of hydrothermal treatments on the structure of a natural zeolite through a combined XRD, FTIR, XRF, SEM and N<sub>2</sub>-porosimetry analysis", *Microporous and Mesoporous Materials*, 134(1-3): 29-43, (2010).
- [13] Gottardi, G., and Galli, E., *Natural zeolites*, Springer, Berlin, (1985).
- [14] Mumpton, F. A., "Clinoptilolite redefined", *American Mineralogist*, 45(3-4): 351-369, (1960).
- [15] Smyth, J. R., Spaid, A. T., and Bish, D. L., "Crystal structures of a natural and a Cs-exchanged clinoptilolite", *American Mineralogist*, 75: 522–528, (1990).
- [16] Ackley, M. W., Giese, R. F., and Yang, R. T., "Clinoptilolite: Untapped potential for kinetics gas separations", *Zeolites*, 12(7): 780-788, (1992).
- [17] Jayaraman, A., Yang, R. T., Chinn, D., and Munson, C. L., "Tailored clinoptilolites for nitrogen/methane separation", *Industrial & Engineering Chemistry Research*, 44(14): 5184-5192, (2005).
- [18] Kennedy, D. A., and Tezel, F. H., "Cation exchange modification of clinoptilolite – Screening analysis for potential equilibrium and kinetic adsorption separations involving methane, nitrogen, and carbon dioxide", *Microporous and Mesoporous Materials*, 262: 235-250, (2018).
- [19] Ghahri, A., Golbabaie, F., Vafajoo, L., Mireskandari, S. M., Yaseri, M., and Shahtaheri, S. J., "Removal of Greenhouse Gas (N<sub>2</sub>O) by Catalytic Decomposition on Natural Clinoptilolite Zeolites Impregnated with Cobalt", *International Journal of Environmental Research*, 11: 327-337, (2017).
- [20] Karousos, D. S., Sapalidis, A. A., Kouvelos, E. P., Romanos, G. E., and Kanellopoulos, N. K., "A study on natural clinoptilolite for CO<sub>2</sub>/N<sub>2</sub> gas separation", *Separation Science and Technology*, 51(1): 83-95, (2016).
- [21] Macala, J., Pandova, I., and Panda, A., "Clinoptilolite as a mineral usable for cleaning of exhaust gases", *Gospodarka Surowcami Mineralnymi-Mineral Resources Management*, 25(4): 23-32, (2009).
- [22] Meimand, M. M., Javid, N., and Malakootian, M., "Adsorption of Sulfur Dioxide on Clinoptilolite/Nano Iron Oxide and Natural Clinoptilolite", *Health Scope*, 8(2): e69158, (2019).

- [23] Pour, A. A., Sharifnia, S., NeishaboriSalehi, R., and Ghodrati, M., "Performance evaluation of clinoptilolite and 13X zeolites in CO<sub>2</sub> separation from CO<sub>2</sub>/CH<sub>4</sub> mixture", *Journal of Natural Gas Science and Engineering*, 26: 1246-1253, (2015).
- [24] Yasyerli, S., Ar, I., Dogu, G., and Dogu, T., "Removal of hydrogen sulfide by clinoptilolite in a fixed bed adsorber", *Chemical Engineering and Processing-Process Intensification*, 41(9): 785-792, (2002).
- [25] Allen, S. J., Ivanova, E., and Koumanova, B., "Adsorption of sulfur dioxide on chemically modified natural clinoptilolite", *Acid modification. Chemical Engineering Journal*, 152(2-3): 389-395, (2009).
- [26] Christidis, G. E., Moraetis, D., Keheyani, E., Akhalbedashvili, L., Kekelidze, N., Geworkyan, R., Yeritsyan, H., and Sargsyan, H., "Chemical and thermal modification of natural HEU-type zeolitic materials from Armenia, Georgia and Greece", *Applied Clay Science*, 24(1-2): 79-91, (2003).
- [27] Ates, A., and Hardacre, C., "The effect of various treatment conditions on natural zeolites: Ion exchange, acidic, thermal and steam treatments", *Journal of Colloid and Interface Science*, 372(1): 130-140, (2012).
- [28] Rozic, M., Cerjan-Stefanovic, S., Kurajica, S., Maefat, M. R., Margeta, K., and Farkas, A., "Decationization and dealumination of clinoptilolite tuff and ammonium exchange on acid-modified tuff", *Journal of Colloid and Interface Science*, 284(1): 48-56, (2005).
- [29] Erdoğan Alver, B., "A comparative adsorption study of C<sub>2</sub>H<sub>6</sub> and SO<sub>2</sub> on clinoptilolite-rich tuff: Effect of acid treatment", *Journal of Hazardous Materials*, 262: 627-633, (2013).
- [30] Amon, M., Dobeic, M., Sneath, R. W., Phillips, V. R., Misselbrook, T. H., and Pain, B. F., "A farm-scale study on the use of clinoptilolite zeolite and De-Odorase® for reducing odour and ammonia emissions from broiler houses", *Bioresource Technology*, 61(3): 229-237, (1997).
- [31] Bernal, M. P., and Lopez-Real, J. M., "Natural zeolites and sepiolite as ammonium and ammonia adsorbent materials", *Bioresource Technology*, 43(1): 27-33, (1993).
- [32] Bernal, M. P., Lopez-Real, J. M., and Scott, K. M., "Application of natural zeolites for the reduction of ammonia emissions during the composting of organic wastes in a laboratory composting simulator", *Bioresource Technology*, 43(1): 35-39, (1993).
- [33] Caputo, D., de Gennaro, B., Liguori, B., Pansini, M., and Colella, C., "Adsorption properties of clinoptilolite-rich tuff from Thrace, NE Greece", *Oxide-based Systems at the Crossroads of Chemistry - Second International Workshop, Como, Italy*, 121-129, (2000).
- [34] Čižhotný, K., Melenová, L., Jirglová, H., Boldiš, M., and Kočířík, M., "Sorption of ammonia from gas streams on clinoptilolite impregnated with inorganic acids", *Studies in Surface Science and Catalysis*, 142: 1713-1720, (2002).
- [35] Helminen, J., Helenius, J., Paatero, E., and Turunen, I., "Adsorption equilibria of ammonia gas on inorganic and organic sorbents at 298.15 K", *Journal of Chemical and Engineering Data*, 46(2): 391-399, (2001).
- [36] Milovanovic, J., Eich-Greatorex, S., Krogstad, T., Rakic, V., and Rajic, N., "The use in grass production of clinoptilolite as an ammonia adsorbent and a nitrogen carrier", *Journal of the Serbian Chemical Society*, 80(9): 1203-1214, (2015).



- [37] Tehrani, R. M. A., and Salari, A. A., "The study of dehumidifying of carbon monoxide and ammonia adsorption by Iranian natural clinoptilolite zeolite", *Applied Surface Science*, 252(3): 866-870, (2005).
- [38] Radosavljevic-Mihajlovic, A. S., Dondur, V. T, Daković, A., Lemic J. B., and Tomasevic-Canovic, M. R., "Physicochemical and structural characteristics of HEU-type zeolitic tuff treated by hydrochloric acid", *Journal of the Serbian Chemical Society*, 69(4): 273-282, (2004).
- [39] Arcoya, A., González, J., Travieso, N., and Seoane, X., "Physicochemical and catalytic properties of a modified natural clinoptilolite", *Clay Minerals*, 29(1): 123-131, (1994).
- [40] Moore, D. M., and Reynolds Jr. R. C., *X-ray Diffraction and the Identification and Analysis of Clay Minerals*. Oxford University Press, Oxford, (1989).
- [41] Esenli F., and Sirkecioğlu A. "The relationship between zeolite (heulandite-clinoptilolite) content and the ammonium-exchange capacity of pyroclastic rocks in Gördes, Turkey." *Clay Minerals*, 40: 557-564, (2005).
- [42] De Man, A. J. M., Ueda, S., Annen, M. J., Davis. M. E., and Van Santen. R. A. "The stability and vibrational spectra of three-ring containing zeolitic silica polymorphs, *Zeolites*, 12(7): 789-800, (1992).
- [43] Akdeniz, Y., Ülkü, S., "Thermal stability of Ag-exchanged clinoptilolite rich mineral, *Journal of Thermal Analysis and Calorimetry*, 94(3): 703-710, (2008).
- [44] Salvestrini, S., Sagliano, P., Iovino, P., Capasso, S., and Colella, C., "Atrazine adsorption by acid-activated zeolite-rich tuffs", *Applied Clay Science*, 49(3): 330-335, (2010).
- [45] Rodríguez-Fuentes, G., Ruiz-Salvador, A. R., Mir, M., Picazo, O., Quintana, G., and Delgado, M., "Thermal and cation influence on ir vibrations of modified natural clinoptilolite", *Microporous and Mesoporous Materials*, 20(4-6): 269-281, (1998).
- [46] Dziejdzicka, A., Sulikowski, B., and Ruggiero-Mikołajczyk, M., "Catalytic and physicochemical properties of modified natural clinoptilolite", *Catalysis Today*, 259: 50-58, (2016).
- [47] Deka, R. C., "Acidity in zeolites and their characterization by different spectroscopic methods", *Indian Journal of Chemical Technology*, 5: 109-123, (1998).
- [48] Bucko, T., and Benco, L., "Adsorption and vibrational spectroscopy of ammonia at mordenite: Ab initio study", *The Journal of Chemical Physics*, 120(21): 10263-10277, (2004).
- [49] Lercher, J. A., Gründling, C., and Eder-Mirth, G., "Infrared studies of the surface acidity of oxides and zeolites using adsorbed probe molecules", *Catalysis Today*, 27(3-4): 353-376, (1996).
- [50] Zecchina A., Marchese L., Bordiga, S., Pazè, C., and Gianotti E., "Vibrational Spectroscopy of NH<sub>4</sub><sup>+</sup> Ions in Zeolitic Materials: An IR Study", *The Journal of Physical Chemistry B*, 101(48): 10128-10135. (1997).
- [51] Nakamoto, K., *Infrared and Raman Spectra of Inorganic and Coordination Compounds Part A: Theory and Applications in Inorganic Chemistry*, Sixth Edition, A John Wiley & Sons, Inc., Publication Hoboken, New Jersey, (2008).
- [52] Lowell S., Shields J. E., Thomas M. A. and Thommes M., *Characterization of Porous Solids and Powders: Surface Area, Pore Size and Density*, Kluwer Academic Publishers, Dordrecht, Netherlands, (2004).

- [53] Sing K. S. W., Everett D. H., Haul R. A. W., Moscou L., Pierotti R. A., Rouquerol J., and Siemieniewska T., "Reporting physisorption data for gas/solid systems with Special Reference to the Determination of Surface Area and Porosity", *Pure and applied chemistry*, 57(4): 603-619, (1985).
- [54] Reddy, K. S. N., Eapen, M. J., Soni, H. S., and Shiralkar, V. P., "Sorption properties of cation-exchanged beta zeolites", *The Journal of Physical Chemistry*, 96: 7923-7928, (1992).
- [55] Garcia-Basabe, Y., Rodriguez-Iznaga, I., de Menorval, L. C., Llewellyn, P., Maurin, G., Lewis, D. W., Binions, R., Autie, M., and Ruiz-Salvador, A. R., "Step-wise dealumination of natural clinoptilolite: Structural and physicochemical characterization", *Microporous and Mesoporous Materials*, 135(1-3): 187-196, (2010).
- [56] Cakicioglu-Ozkan, F., and Ulku, S., "The effect of HCl treatment on water vapor adsorption characteristics of clinoptilolite rich natural zeolite", *Microporous and Mesoporous Materials*, 77(1): 47-53, (2005).
- [57] Wang, X., and Nguyen, A. V., "Characterisation of electrokinetic properties of clinoptilolite before and after activation by sulphuric acid for treating CSG water", *Microporous and Mesoporous Materials*, 220: 175-182, (2016).
- [58] Ciahotný, K., Melenová, L., Jirglová, H., Pachtová, O., Kočířík, M., and Eić, M., "Removal of ammonia from waste air streams with clinoptilolite tuff in its natural and treated forms", *Adsorption*, 12: 219-226, (2006).
- [59] Król, M., "Natural vs. Synthetic Zeolites", *Crystals*, 10(7): 622-630, (2020).